DC Voltage Control and Power-Sharing of Multi-Terminal DC Grids Based on Optimal DC Power Flow and Voltage Droop Strategy

F. Azma* and H. Rajabi Mashhadi*(C.A.)

Abstract: This paper develops an effective control framework for DC voltage control and power-sharing of Multi-Terminal DC (MTDC) grids based on an Optimal Power Flow (OPF) procedure and the voltage-droop control. In the proposed approach, an OPF algorithm is executed at the secondary level to find optimal reference of DC voltages and active powers of all voltage-regulating converters. Then, the voltage droop characteristics of voltage-regulating converters, at the primary level, are tuned based on the OPF results such that the operating point of the MTDC grid lies on the voltage droop characteristics. Consequently, the optimally-tuned voltage droop controller leads to the optimal operation of the MTDC grid. In case of variation in load or generation of the grid, a new stable operating point is achieved based on the voltage droop characteristics. By execution of a new OPF, the voltage droop characteristics are re-tuned for optimal operation of the MTDC grid after the occurrence of the load or generation variations. The results of simulation on a grid inspired by CIGRE B4 DC grid test system demonstrate efficient grid performance under the proposed control strategy.

Keywords: CIGRE B4 DC Grid Test System, Hierarchical Control, Multi-Terminal DC Grids, Optimal Power Flow, Voltage Droop Control.

1 Introduction

Recently, a lot of attentions have been focused, both from the industry pioneers and academia, towards the concept of DC grids. From 1951 till now, more than 180 mainly two-terminal HVDC projects have been put into operation around the world. Over the past 20 years some HVDC applications have been expanded with two or three terminals in order to obtain the first functional Multi-Terminal DC (MTDC) grids [1]. With the development and increasing availability from multiple vendors of high power voltage source converters (VSC), the prospect of a MTDC grid, composed of multiple converters has become a realistic possibility [2].

Numerous advantages and application ideas have been identified and proposed in the literature with regards to the MTDC concept. According to [3], MTDC grids could be one of the most suitable solutions for integration of wind farm energy into the mainland AC grids. Furthermore, MTDC grids could facilitate the development of the so-called European super grid [4], [5]. Ultimately this large MTDC would interconnect the North Sea wind farms with Mediterranean solar plants and Scandinavian hydropower. Besides, MTDC applications can be found for interconnecting multiple non-synchronous AC areas [6].

The need for MTDC networks and the advantages they could bring for the modern grids are already well-established. However, at the moment the knowledge on the subject is scarce. Several proposals for primary control of DC voltage can be found in the literature, as the ones in [1, 7, 8] and [9], all of them presenting various advantages and disadvantages. At the present moment, the concept of MTDC still requires a lot of researches on the topics related to hierarchical control, protection, as well as markets and interacting with existing AC networks.

This paper provides a control framework based on an optimal DC power flow algorithm and the voltage droop strategy for efficient control and power-sharing in MTDC grids. In the proposed control framework, the voltage droop characteristics are tuned based on the optimal DC power flow results. Hence, the grid is efficiently controlled under voltage-droop scheme in case of variations in demand and generation.

Iranian Journal of Electrical & Electronic Engineering, 2015.
Paper first received 16 Apr. 2014 and in revised form 20 Oct. 2014.
* The Authors are with the Department of Electrical Engineering, Ferdowsi University of Mashhad Mashhad, Iran.
E-mails: F.Azma@ieee.org and h_mashhadi@um.ac.ir.

The rest of this paper is organized as follows. Section 2 presents the optimal DC power flow algorithm. The proposed control framework, composed of optimal power flow and voltage droop control, is presented in Section 3. The simulation results on CIGRE B4 DC grid test system are reported in Section 4. The paper conclusions are presented in Section 5.

2 Optimal DC Power Flow Algorithm

2.1 Optimal DC Power Flow: Problem Statement

Considering an MTDC grid with *N* DC terminals (or DC buses), the problem of DC optimal power flow (DCOPF) for a DC grid is formulated by Eqs. (1)-(5), stated below,

$$\min_{\mathbf{V}} f\left(\mathbf{V}\right) \tag{1}$$

subject to the following constraints,

$$\mathbf{g}\left(\mathbf{V},\mathbf{P}\right)=0 \tag{2}$$

$$V_{DC}^{\min} < V_{DC,i} < V_{DC}^{\max}, i=1,\ldots,N \tag{3}$$

$$\left|P_i\right| < P_i^{\max}, i=1,\ldots,N \tag{4}$$

$$\left|I_{DC,k}\right| < I_{DC,k}^{\max}, k=1,\ldots,L \tag{5}$$

The objective function and constraints of the optimal DC power flow problem, outlined by Eqs. (1)-(5), are explained below.

In Eq. (1), f indicates the grid losses, which have to be minimized. Moreover, $\mathbf{V}$ is the vector of grid's DC voltages, as stated below,

$$\mathbf{V}=\left[V_{DC,1}V_{DC,2}\ldots V_{DC,N}\right]^T \tag{6}$$

The minimization function f can be computed as,

$$f\left(\mathbf{V}\right)=\sum_{i=1}^{N}\sum_{j=(i+1)}^{N}G_{ij}\left(V_i-V_j\right)^2+\sum_{i=1}^{N}G_{ii}V_i^{\,2} \tag{7}$$

where, G_{ij} indicates the total conductance between terminals *i* and *j* while G_{ii} represents the sum of all conductances connected between the terminal *i* and the ground.

Constraint (2) includes mismatch between generation and demand and imposes DC load flow equations, as follows,

$$\mathbf{g}\left(\mathbf{V},\mathbf{P}\right)=\left[g_1\ g_2\ \ldots\ g_N\right]^T \tag{8}$$

where,

$$\mathbf{P}=\left[P_1\ P_2\ \ldots\ P_N\right]^T \tag{9}$$

is the vector of grid's powers,

$$g_i=P_{Gi}-P_{Li}+\sum_{j=1}^{N}G_{ij}V_iV_j \tag{10}$$

and, P_{Gi} and P_{Li} represent the generation and load at terminal *i*. Constraints (3)-(5) indicate the limits on DC terminals voltages, the power flowing through converters and DC current through the DC transmission lines. In constraint (3), $V_{DC}^{\max}$ and $V_{DC}^{\min}$ indicate the upper and lower limits on DC voltages at grid's terminals, respectively. In Eq. (4), $P_i^{\max}$ indicates the maximum permissible power of the converter station *i*. Finally, $I_{DC,k}^{\max}$ in Eq. (5) sets the upper limit on the permissible DC current transmitted by DC link *k*.

It is worth noting that two types of DC buses can be identified in a DC grid system, as expressed below,

- Load (generation) or P-bus, whose net injected power is pre-determined.
- Voltage or slack bus whose DC voltage is pre-specified.

2.2 Optimal DC Power Flow: Solution Method

The optimal DC power flow problem, stated by Eqs. (1)-(5), represents a nonlinear-constrained optimization problem which will be solved using a gradient-based optimization technique. This is done by constructing the Lagrangian for the optimization problem, as stated below,

$$L\left(\mathbf{V},\mathbf{P}\right)=f\left(\mathbf{V}\right)+\boldsymbol{\lambda}^{\mathrm{T}}\mathbf{g}\left(\mathbf{V},\mathbf{P}\right)+\mathbf{q}\left(\mathbf{V},\mathbf{P},\mathbf{I}\right) \tag{11}$$

where, $\boldsymbol{\lambda}$ is a vector containing Lagrange multipliers for the equality constraint (2), $\mathbf{I}$ is the vector of DC currents through grid DC links, $\mathbf{q}$ is the penalty function for the inequality constraints of (3)-(5), stated below,

$$\begin{aligned}\mathbf{q}\left(\mathbf{V},\mathbf{P},\mathbf{I}\right)=&\sum_{i=1}^{N}pf_{v^{\max},i}\left(V_i-V_i^{\max}\right)^2\\&+\sum_{i=1}^{N}pf_{V^{\min},i}\left(V_i-V_i^{\min}\right)^2\\&+\sum_{i=1}^{N}pf_{P,i}\left(P_i-P_i^{\min}\right)^2\\&+\sum_{k=1}^{L}pf_{I,k}\left(I_{DC,k\,i}-I_{DC,i}^{\max}\right)^2\end{aligned} \tag{12}$$

in which $pf_{v^{\max},i}$, $pf_{v^{\min},i}$, $pf_{P,i}$, and $pf_{I,i}$ denote the penalty factors for maximum DC voltage limits, minimum DC voltage limits, converters power limits and DC links current limits, respectively.

The solution of the optimal DC power flow can be obtained by setting the Lagrangian derivative with respect to the unknown variables to zero and then solving the problem iteratively.

3 Proposed Control Framework

The proposed control framework is based on the optimal DC power flow and the voltage droop strategy. To be more specific, the voltage droop characteristics of the voltage regulating stations are tuned based on the optimal DC power flow results. Fig. 1 depicts the structure of the proposed control framework. The

illustrated structure includes a high-level secondary control center (SCC) which sends appropriate control signals (i.e. α, β and γ) to the control system of the converter stations at the primary level. In fact, the optimal DC power flow is carried out in the secondary control level while voltage-droop control for each converter station is performed locally and at the primary level. It is worth noting that the decoupled current control (or *d-q* control) strategy [10] is implemented at the primary level.

3.1 Optimal Power Flow-Based DC Voltage Control and Power-Sharing

The general structure of the proposed control framework, including primary and secondary levels, for the MTDC grids was presented and discussed in Section II. In the proposed hierarchical structure, the secondary level sets the reference power in the voltage-droop characteristic and hence guarantees the desirable power exchange.

At the primary control level, however, voltage droop control strategy is employed. In this strategy, the voltage-regulating converters contribute to the DC voltage control and power sharing in the grid based on their voltage droop characteristics. Fig. 2 illustrates the general form of a voltage droop characteristic. This characteristic can be expressed mathematically by,

$$\alpha V_{DC} + \beta P + \gamma = 0 \tag{13}$$

where, V_{DC} and P are voltage and power at the DC-side of the converter and the PCC, respectively and α, β and γ are the coefficients of the voltage droop characteristics, determined by the secondary control level, as shown in Fig. 3.

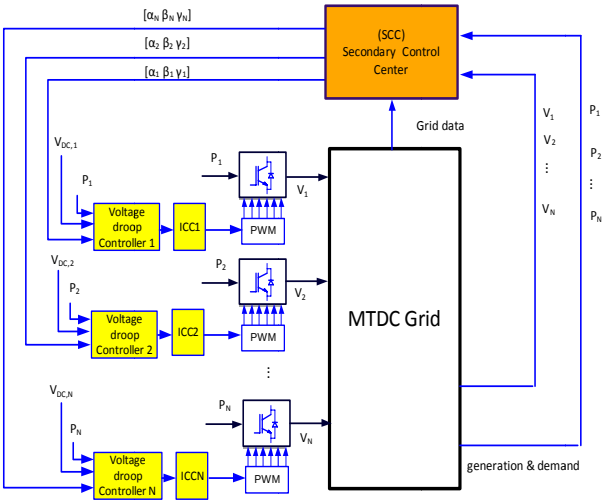

Fig. 1 The overall control structure for an MTDC grid with primary and secondary control levels with voltage droop characteristics.

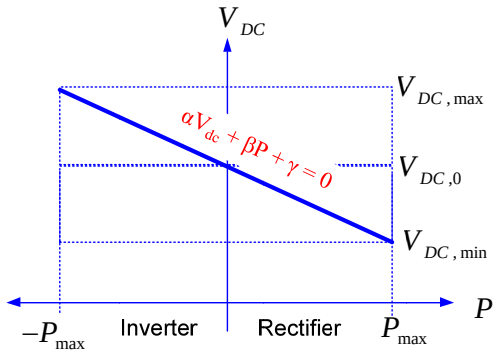

Fig. 2 The generalized voltage droop characteristics.

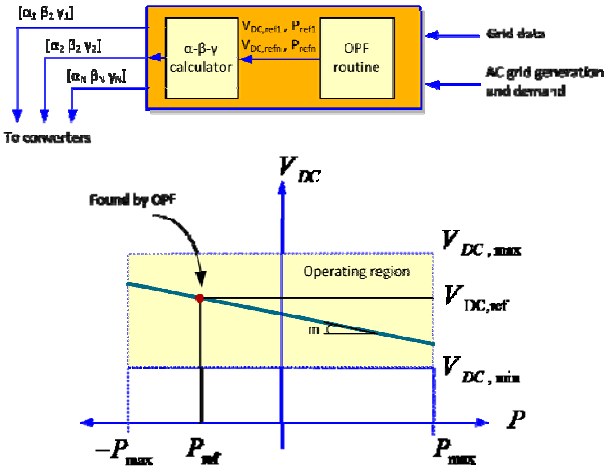

Fig. 3 Adjustment of voltage droop characteristic coefficients based on the optimal DC power flow solution.

The secondary control level adjusts these coefficients for the voltage-regulating converters based on the power exchange requirements and optimal DC power flow outputs.

To be more specific, the coefficients of the voltage characteristics are set using optimal DC power flow outputs ($V_{DC,ref}$ and P_{ref}). In other word, α, β and γ must be selected such that the $V_{DC,ref}$ and P_{ref} lie on the voltage droop characteristics of the voltage regulating converters.

Hence, for k voltage-regulating converters, the $V_{DC,ref}$ and P_{ref} obtained from optimal power flow solution must lie on the corresponding voltage characteristics,

$$\alpha_i V_{DC,ref,i} + \beta_i P_{ref,i} + \gamma_i = 0,\ i = 1,\ldots,k \tag{14}$$

where, $V_{DC,ref,i}$ and $P_{ref,i}$ indicate the reference DC voltage and power of the voltage-regulating station i (derived from optimal DC power flow), respectively, and α_i, β_i and γ_i are the voltage droop coefficients of the voltage-regulating station i.

There are three unknown parameters in Eq. (14) (α_i, β_i and γ_i). Hence, two more equations must be added to solve for α_i, β_i and γ_i. In this paper, the slope of voltage droop characteristics, m_i, are assumed constant and pre-defined. Accordingly,

$$m_i = \frac{\beta_i}{\alpha_i},\ i = 1,\ldots,k \tag{15}$$

Assuming $\alpha_i = 1$, one can compute,

$$\beta_i = m_i,\ i = 1,\ldots,k \tag{16}$$

Based on Eqs. (15) and (17), the γ_i can be determined as,

$$\gamma_i = -V_{DC,ref,i} - m_i P_{ref,i},\ i = 1,\ldots,k \tag{17}$$

By tuning the voltage droop coefficients using Eqs. (15)-(17), it's guaranteed that the grid with voltage-droop control will operate on the efficient operating-point obtained by the optimal DC power flow. The procedure of tuning the voltage droop characteristics based on optimal DC power flow solution is illustrated in Fig. 3.

It must be noted that in the proposed approach, it's not necessary to include voltage-droop characteristics directly into optimal DC power flow algorithm. The voltage droop coefficients are tuned based on power flow results.

3.2 Frequency Support to the AC Grids

In case of weak AC systems, the MTDC grid can be helpful to support the frequency of such a grid. This can be accomplished by including a frequency-regulating block in the outer control loop of the *d-q* control strategy. This is depicted in Fig. 4. In fact, the reference power for the outer active power controller is determined based on the voltage droop characteristic as well as the frequency controller action.

By applying the frequency support action, the MTDC grid would aid the weak AC system in balancing the generation and consumption through the time. Based on Fig. 4, the change in reference power of frequency controlling VSC, in Laplace domain, is governed by,

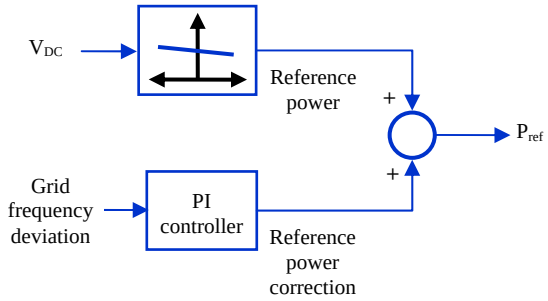

Fig. 4 Implementation of frequency controller in the outer loop of *d-q* control strategy.

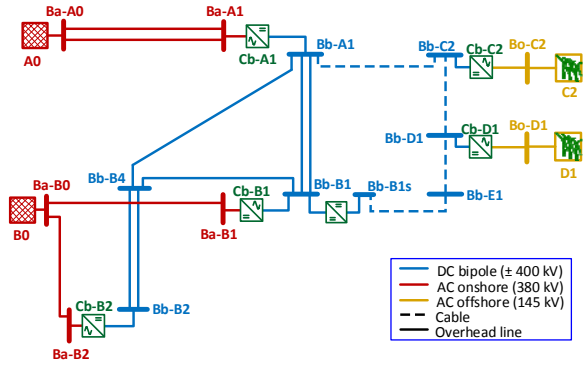

Fig. 5 Schematic diagram of DCS3.

$$\Delta P_{ref}(s) = mV_{DC}(s) + \Delta f(s)\left(k_{f,P} + {}^{k_{f,I}}\!/_{s}\right) \tag{18}$$

where, m is droop slope, Δf represents frequency deviation of the AC system, and $k_{f,P}$ and $k_{f,I}$ indicate proportional and integral gain of the frequency support controller, respectively, shown in Fig. 4.

4 Simulation Results

The proposed control framework is evaluated by the recently released CIGRE B4 DC grid test system. The CIGRE test system has been developed by CIGRE's B4 working group as a benchmark for conducting DC grids studies and analysis. The CIGRE B4 DC grid test system includes two onshore AC systems, four offshore AC systems, two DC nodes, with no connection to any AC system and three DC systems, namely DCS1, DCS2, and DCS3. The overall system is comprised of 11 VSC stations.

In this paper the DCS3, a five-terminal bipolar HVDC meshed grid with DC link voltage of ±400kV, is employed for evaluating the proposed control strategy. In this test grid, shown in Fig. 5, two VSCs are connected to offshore AC buses Bo-C2 and B0-D1, while other three VSCs serve as interfaces between the DC grid and onshore AC buses Ba-A1, Ba-B1, and Ba-B2 (i.e. are operated as grid connected VSCs).

In DCS3, the offshore systems are modeled as constant power sources and onshore systems are stiff grids represented by ideal voltage sources behind the impedance. It must be noted that two of the AC buses (Ba-B1 and Ba-B2) are stiff grids while the third one (Ba-A1) is considered a weak AC system. DC line and converter stations data are presented in Tables 1 and 2, respectively.

Table 1 overhead line and cable data.

Line Data	R [Ω/km]	L [mH/km]	C [μF/km]	G [μS/km]
DC OHL±400 kV	0.0114	0.9356	0.0123	-
DC Cable±400 kV	0.0095	2.1120	0.1906	0.048
AC OHL 380 kV	0.0200	0.8532	0.0135	-

Table 2 converter station parameters.

VSC Station	R_T (Ω)	L_T (mH)	C (μF)
Cb-A1	0.403	33	450
Cb-B1	0.403	33	450
Cb-B2	0.403	33	450
Cb-C2	1.210	98	150
Cb-D1	0.65	49	300

The control mode of VSCs depends on whether they are connected to an offshore or an onshore AC grid. The grid-side converters, Cb-B1 and Cb-B2, control the DC voltage of the MTDC grid (or the active power at the PCC) and reactive power at the PCC, as they are connected to stiff grids. On the other hand, the VSC Cb-A1, connected to the weak AC grid Ba-A1, supports the frequency of the AC grid and controls amplitude of the AC voltage at the PCC.

During the simulations, it is assumed that the onshore converter stations Cb-A1 and Cb-B2 demand fixed power while Cb-B1 acts as the slack converter (i.e. Bb-B1 is the DC slack bus). The voltage droop characteristics of these three stations are adjusted by the optimal DC power flow such that the mentioned requirements (i.e. fixed power demand by Cb-A1 and Cb-B2) are met. More detailed data on the optimal DC power flow are presented in Table 3. Note that the base power is 500 MW and sampling time for the SCC is assumed one second.

Table 3 Base-Case power flow data.

DC Bus	Bus Type	DC Voltage	Net Injected Power
Bb-A1	P	Unknown	-0.8
Bb-B1	Slack	Unknown	Unknown
Bb-B1s	intermediate	Unknown	0
Bb-B2	P	Unknown	-0.4
Bb-B4	intermediate	Unknown	0
Bb-C2	P	Unknown	0.9
Bb-D1	P	Unknown	1.9
Bb-E1	intermediate	Unknown	0

Table 4 Power Flow Results for the Base-Case.

DC Bus	Bus type	DC Voltage (pu)	Net Power (pu)
Bb-A1	P	0.9534	-0.80
Bb-B1	Slack	0.9520	-1.54
Bb-B1s	intermediate	0.9513	0
Bb-B2	P	0.9502	-0.40
Bb-B4	intermediate	0.9578	0
Bb-C2	P	0.9603	0.90
Bb-D1	P	0.9561	1.90
Bb-E1	intermediate	0.9534	0

Table 5 Voltage Droop Parameters for the Base-Case.

Converter Station	α	β	γ
Bb-A1	1	0.04	-0.940
Bb-B1	1	0.02	-0.939
Bb-E1	1	0.03	-0.945

4.1 Base-Case Simulation

The base-case simulation is carried out based on the DCOPF data summarized in Table 3. The simulation starts by adjusting the voltage droop characteristics of the grid-side VSCs based on the results of the optimal DC power flow, presented in Table 4. Moreover, the calculated droop coefficients of the grid-side VSCs are also summarized in Table 5. More detailed results of the DCOPF for the base case are shown in Fig. 6. Note that Cb-B1, as the slack converter, has lowest voltage droop slope and hence will have the largest contribution to the power-sharing and DC voltage control of the grid.

The DC voltage and active power profiles for all converter stations, obtained by applying DCOPF-tuned voltage droop characteristics, are illustrated in Figs. 7 and 8, respectively. Moreover, to show the desirable effect of the proposed control technique on grid losses, a comparison between DCS3's losses due to the DCOPF algorithm and a simple DC power flow (DCPF) algorithm is shown in Fig. 9. Note that in the DCPF algorithm, the voltage of the slack bus (i.e. Bb-B1) is assumed 1 pu.

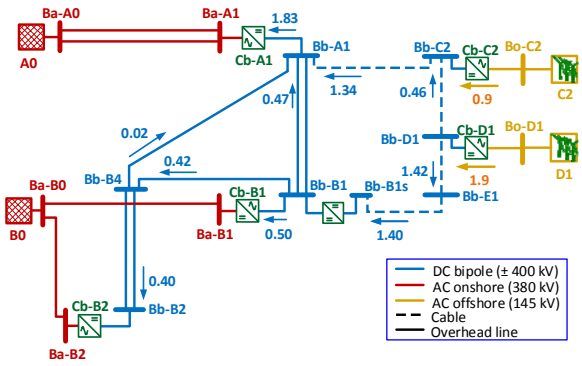

Fig. 6 Detailed optimal DC power flow results for base case.

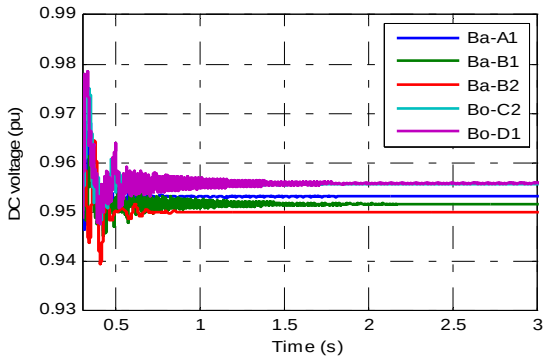

Fig. 7 DC voltages at converter stations for the base case.

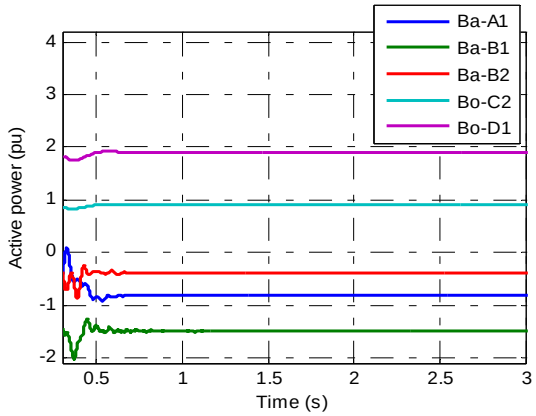

Fig. 8 Active powers at converter stations for the base case.

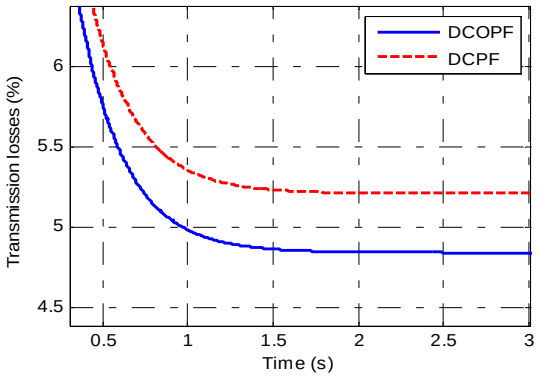

Fig. 9 Transmission losses in MTDC grid for the base-case.

4.2 Variations in Offshore Generation

The second simulation case addresses variations in offshore generations. This simulation is intended to demonstrate how the proposed control approach deals with variations in offshore generation and how new optimal operating point of the grid is achieved.

In this simulation, generation of offshore DC buses, Bb-C2 and Bb-D1 is according to Table 4, prior to t = 0.3 sec. However, at t = 0.3 sec. offshore generation of Bb-D1 is reduced from 1.9 to 1.3 pu. This would results in an instantaneous power imbalance within the grid and the control system must respond to it properly. The DC voltage and active power profiles for this case are depicted in Figs. 10 and 11, respectively. Suddenly after this change in the offshore generation, the voltage droop control of the grid-side converters (i.e. primary control action) start to restore the power balance in the grid. This can be observed in Fig. 11. However, due to such primary control actions, the power flow within the grid deviates from the pre-specified settings. For instance, the power absorbed by Bb-B2 deviates from -0.4 to -0.2. Next, the SCC sends new parameters of the voltage droop characteristics of the grid-side VSCs after about one second, which is its sampling period. This secondary control action restores the pre-specified power flow in the grid.

Besides, as stated earlier, the AC grid Ba-A1 is assumed a weak grid equipped with frequency support control. The frequency controller keeps the frequency of the Ba-A1 at 50 Hz during the variation in the offshore generation and as well as during the modification of the parameters of the voltage droop characteristics by the SCC, as shown in Fig. 12. Moreover, DC transmission losses during this simulation are illustrated in Fig. 13.

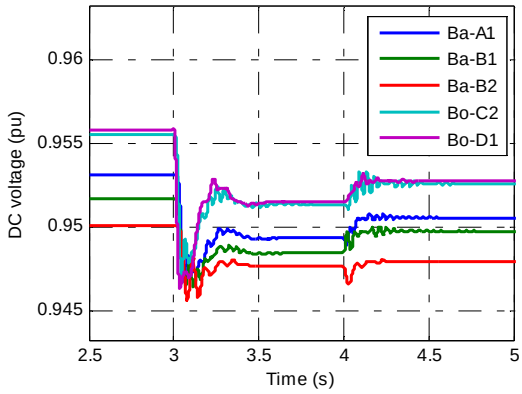

Fig. 10 DC voltages at converter stations for variation in offshore generation.

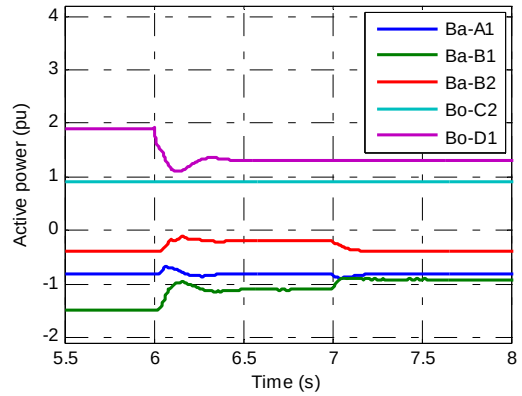

Fig. 11 Active powers at converter stations for variation in offshore generation.

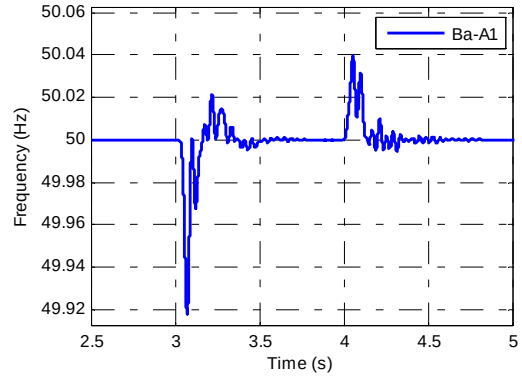

Fig. 12 Frequency at Ba-A1 during variation in offshore generation.

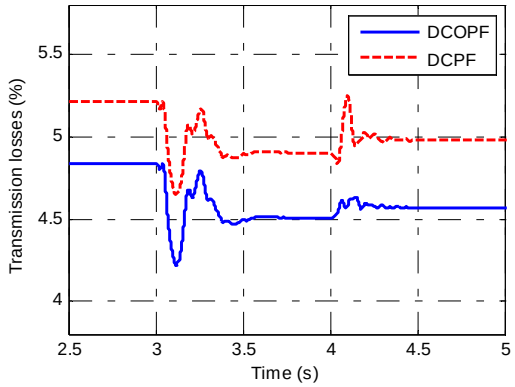

Fig. 13 Transmission losses in MTDC grid during variation in offshore generation.

4.3 Lack of Generation in Weak AC Grid

In the third simulation case, response of the proposed control system to the lack of generation in the weak AC grid, i.e. Ba-A1 is investigated. During this simulation, the demand of Ba-A1 is increased at t = 6 sec, resulting in generation lack of about 0.6 pu. The DC voltages and active powers of the VSC stations during this simulation are shown in Figs. 14 and 15, respectively.

Suddenly after this incident, the net power import by the corresponding VSC, i.e. Cb-A1 is increased due to its frequency support action as well as the voltage droop control of Cb-B1 and Cb-B2. However, the power flow within the grid changes due to these actions. After one second, the SCC sends new parameters of the voltage droop characteristics at t = 7 sec and restores the power flow to the pre-specified values, as shown in Fig. 15.

The frequency of the Ba-A1 during these evolutions is shown in Fig. 16. Clearly, the frequency support action has successfully maintains weak AC grid frequency at the reference level.

Finally, DC transmission losses in this case is shown in Fig. 17 and compared to the losses due to implementation of DC power flow algorithm.

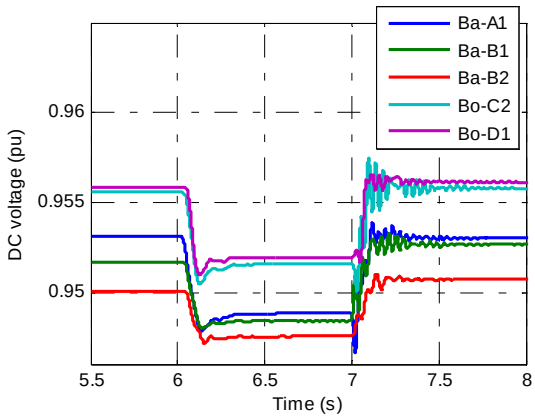

Fig. 14 DC voltages at converter stations during lack of generation in Ba-A1.

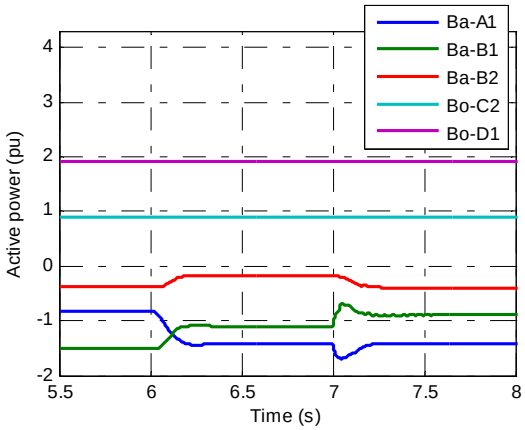

Fig. 15 Active powers at converter stations during lack of generation in Ba-A1.

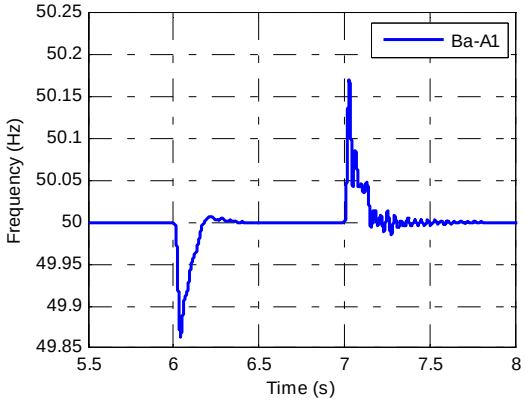

Fig. 16 Frequency at Ba-A1 during lack of generation in Ba-A1.

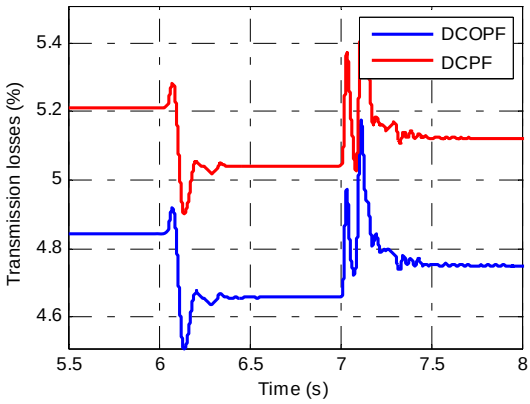

Fig. 17 Transmission losses in MTDC grid during lack of generation in Ba-A1.

5 Conclusion

This paper proposed an optimal power flow-based voltage droop control for efficient control and power-sharing in multi-terminal DC (MTDC) grids based on optimal power flow (OPF) procedure and voltage droop control. In the proposed approach, an OPF algorithm is

executed at the secondary level to find optimal reference DC voltages and active powers of all voltage-regulating converters. Then, the parameters of the voltage droop characteristics of voltage-regulating converters, at the primary level, are tuned based on the OPF results such that the operating point of the MTDC grid lies on the voltage droop characteristics. Consequently, the generalized voltage droop controller leads to the optimal operation of the MTDC grid. In case of variation in load or generation of the grid, a new stable operating point is achieved based on the voltage characteristics. By execution of a new OPF, the voltage characteristics are re-tuned for optimal operation of the MTDC grid after the occurrence of the load or generation variations. The simulation results of CIGRE B4 DC grid test system indicated efficient grid performance under the proposed control strategy. It is worth noting that a low-bandwidth communication channel is necessary between the control levels. However, if the communication between the primary and secondary control center is lost, the DC grid will remain stable based on the previous droop settings, achieving a non-optimal point of operation.

References

[1] K. Meah and A. H. M. S. Ula, "A new simplified adaptive control scheme for multi-terminal HVDC transmission systems," *International Journal of Electrical Power & Energy Systems*, Vol. 32, No. 4, pp. 243–253, May 2010.

[2] C. D. Barker and R. Whitehouse, "Autonomous converter control in a multi-terminal HVDC system", *9th IET International Conference on AC and DC Power Transmission, 2010. ACDC*, pp. 1–5, 2010.

[3] L. Xu, B. W. Williams and L. Yao, "Multi-terminal DC transmission systems for connecting large offshore wind farms", *IEEE Power and Energy Society General Meeting-Conversion and Delivery of Electrical Energy in the 21st Century*, pp. 1-7, 2008.

[4] R. da Silva, R. Teodorescu and P. Rodriguez, "Multilink DC transmission system for supergrid future concepts and wind power integration", *IET Conference on Renewable Power Generation* (*RPG 2011*), pp. 1-6, 2011.

[5] L. Weimers, "A European DC Super Grid-A Technology Providers View", *Power Systems-HVDC*, 2011.

[6] J. Dai, Y. Phulpin, A. Sarlette and D. Ernst, "Coordinated primary frequency control among non-synchronous systems connected by a multi-terminal high-voltage direct current grid", *IET Generation, Transmission & Distribution*, Vol. 6, No. 2. pp. 99-108, 2012.

[7] C. Dierckxsens, K. Srivastava, M. Reza, S. Cole, J. Beerten and R. Belmans, "A distributed DC voltage control method for VSC MTDC systems", *Electric Power Systems Research*, Vol. 82, No. 1, pp. 54–58, Jan. 2012.

[8] S.-Y. Ruan, G.-J. Li, X.-H. Jiao, Y.-Z. Sun and T. T. Lie, "Adaptive control design for VSC-HVDC systems based on backstepping method", *Electric Power Systems Research*, Vol. 77, No. 5-6, pp. 559–565, 2007.

[9] B. K. Johnson, R. H. Lasseter, F. L. Alvarado and R. Adapa, "Expandable multiterminal DC systems based on voltage droop", *IEEE Transactions on Power Delivery*, Vol. 8, No. 4. pp. 1926–1932, 1993.

[10] R. da Silva, R. Teodorescu and P. Rodriguez, "Multilink DC transmission system for supergrid future concepts and wind power integration", *IET Conference on Renewable Power Generation* (*RPG 2011*), pp. 1–6, 2011.

Fariborz Azma was born in Tehran, Iran, in 1966. He received the B.Sc. degree in electronics engineering from Sharif University of Technology, Tehran, Iran, in 1989; and attended the M.Sc. program in electrical engineering at Ferdowsi University of Mashhad in 1991. He is currently pursuing research assistance at the department of Electrical Engineering, Ferdowsi University of Mashhad, Mashhad, Iran.

Habib RajabiMashhadi was born in Mashhad, Iran, in 1967. He received the B.Sc. and M.Sc. degrees with honor from the Ferdowsi University of Mashhad, both in electrical engineering, and the Ph.D. degree from the Department of Electrical and Computer Engineering of Tehran University, Tehran, Iran, under joint cooperation of Aachen University of Technology, Germany, in 2002. He is as Professor of electrical engineering at Ferdowsi University of Mashhad. His research interests are power system operation and planning, power system economics, and biological computation.